K2-138 and the capture in 1st-order 3P-MMRs

M. Cerioni[1,2] & C. Beaugé[1,2]

[1] *Observatorio Astronómico de Córdoba, UNC, Argentina*
[2] *Instituto de Astronomía Teórica y Experimental, CONICET–UNC, Argentina*

Received: 09 February 2024 / Accepted: 29 May 2024

Resumen / En un estudio reciente presentamos evidencia dinámica en favor de la primera resonancia de movimientos-medios de 3 planetas (3P-MMR) de 1er-orden asociada a un sistema real: K2-138. En este trabajo, expandimos los resultados para mostrar que la región de captura es amplia y suave sobre el espacio de parámetros iniciales, y que acumula significativamente más capturas que la 3P-MMR de orden 0 por la que también cruzan los tripletes en su ruta de migración. Además, vemos que *i*) planetas de períodos cortos, *ii*) masas en el orden de las unidades terrestres, y *iii*) masas similares entre el segundo y tercer planeta, favorecen la captura en la resonancia mencionada. La captura también es favorecida para *i*) discos protoplanetarios menos densos, *ii*) con un mayor gradiente de densidad, *iii*) con una razón de aspecto mayor, y *iv*) con una curvatura más pronunciada.

Abstract / In a recent study, we presented dynamical evidence in favour of the first 1st-order 3-planet mean-motion resonance (3P-MMR) associated with a real system: K2-138. In this work, we expand upon those results to show that the capture domain is wide and smooth over the space of initial parameters, and that it produces significantly more captures than the 0th-order 3P-MMR also encountered by the triplets in their migration path. Additionally, we see that *i*) short period planets, *ii*) of a few Earth masses, and with *iii*) similar masses between the second and third planet, favour a capture in the 1st-order 3P-MMR. This capture is also favoured by having a protoplanetary disk of *i*) lower surface density, *ii*) greater surface density gradient, *iii*) greater aspect ratio, and *iv*) greater flare.

Keywords / planets and satellites: dynamical evolution and stability — planets and satellites: formation — planet–disk interactions

1. Introduction

We have recently presented dynamical evidence suggesting that, during the protoplanetary disk age, the last planetary pair in K2-138 became captured in the 2-planet mean-motion resonance (2P-MMR) 3:1, which was immediately followed by a capture of the last planetary triplet into the 3P-MMR $(2, -4, 3)$ (Cerioni & Beaugé, 2023). Such a scenario, followed by tidal interactions between the star and the planets, can precisely and naturally explain the observed separations between each of the 6 planets and the multiple involved 2P-MMRs, as well as being numerically reproducible with classical migration models (such as Tanaka et al., 2002).

The $(2, -4, 3)$ capture marks the first time a 1st-order 3P-MMR (the order is given by the sum of the indexes) is identified in a real planetary system. In theory, this 3P-MMR should be weaker than other 0th-order resonances which have been repeatedly found in other systems such as TRAPPIST-1, TOI-178 or Kepler-223 (Agol et al., 2021; Leleu et al., 2021; Hühn et al., 2021). The magnitude of a kth-order 3P-MMR is proportional to the kth power of the eccentricities, so 1st-order resonances are generally thought to be too weak to impact real planetary systems.

Although in our previous study we provided 2 numerical integrations that tested different system parameters to show that the capture in the 1st-order resonance was plausible, it was still not clear if it was probable, or just a fortunate selection of finely tuned initial conditions. On the other hand, we know that the capture of the last two planets in the 3:1 2P-MMR could also enable a capture in the $(4, -7, 3)$ 0th-order 3P-MMR. Why is it then that the triplet would end up being captured in the weaker resonance? What determines which 3P-MMR will the triplet converge to after the 3:1 capture?

In this work, we use simulation grids to explore the space of planetary and disk parameters and show which conditions favour a capture in the $(2, -4, 3)$ or $(4, -7, 3)$ 3P-MMRs. Such results will inform a future study that rigorously addresses why a triplet would choose one resonance over the other.

2. The standard system

2.1. Planetary and disk parameters

In order to compare the results upon changing initial conditions, we are going to adopt a standard system of 3 planets with $m_i = (8, 9, 10)$ $M_\oplus$ orbiting around a sub-solar star of 0.75 $M_\odot$. Additionally, we will fix the semimajor axis of the third planet at 1 AU. Each grid cell fixes the initial relative separations, so the other two initial positions can be calculated.

For the protoplanetary disk we follow the one

✉ *Contact* / matias.cerioni@unc.edu.ar

adopted in Set#1 of Cerioni & Beaugé (2023), that is, a Tanaka & Ward (2004) –type disk parametrized by $\Sigma_0 = 100$ gr cm^{-2} and $(s, H_0, f) = (0.5, 0.05, 0)$, which respectively correspond to the surface density at $r = 1$ AU, the radius power of the surface density, the aspect ratio at $r = 1$ AU, and the disk flare.

The effect of the gas disk on the planets will be that of circularization and orbital decay, i.e Type-I planetary migration. The reader can check the aforementioned works for the equations governing these effects.

2.2. Simulation grid parameters

We used the parameters just described to run a grid of simulations in mean-motion-ratio space, i.e $(n_1/n_2, n_2/n_3)$. In K2-138, the outer triplet goes through convergent migration towards the $(3/2\,,\,3/1)$ intersection from greater separations. For this reason, we create a grid of 10×10 cells varying $n_1/n_2 \in [1.54, 1.65]$ and $n_2/n_3 \in [3.3, 3.8]$

We evolve each simulation long enough so that the outer pair can either converge to the 3:1 2P-MMR and become captured in one of the 3P-MMRs, or continue past the 3:1 towards smaller separations.

Lastly, we mention that for these simulations we employ a Bulirsch-Stoer integration scheme with variable timestep and a maximum allowed error of 10^{-11} per integration step (Bulirsch & Stoer, 1966).

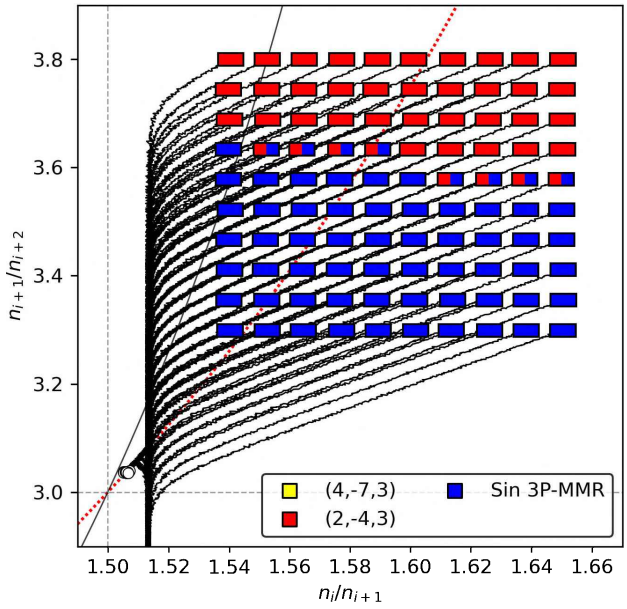

Fig. 1. Simulation grid for our standard system as described in Section 2.1. Boxes mark the initial conditions of the different simulations. Their colors mark their final configuration (see text in Section 3.1 for more details). From them stem the migration routes in black. Diagonal curves correspond to the $(4, -7, 3)$ (black) and $(2, -4, 3)$ (dotted red) 3P-MMRs. White circles mark the final positions of the triplets which ended within plot limits.

3. Results

3.1. Standard system grid

In Fig. 1 we can see the evolution of the simulation grid. Colored boxes mark the initial separations of each system, and from them stem the respective migration routes in black. The diagonal curves that cross the $(3/2\,,\,3/1)$ intersection are the $(4, -7, 3)$ (black) and $(2, -4, 3)$ (dotted red) 3P-MMRs. White circles mark the final positions of those triplets that end up within plot limits. The colors in the boxes indicate the final destination of each triplet. A red box means that the triplet ended up being captured in the $(2, -4, 3)$ 3P-MMR. A yellow one marks a capture in the $(4, -7, 3)$. A blue one indicates that the triplet has crossed the 3:1 2P-MMR without being captured. Mixed-colors indicate a temporal capture towards the right-most color of the box. For example, [red | blue] boxes correspond to a temporal capture in the $(2, -4, 3)$ where the triplet eventually was let go to continue its migration path downwards and past the 3:1.

Every triplet migrates to more compact systems (towards the lower left corner), until the inner pair bumps into the 3:2 resonance, although with a visible offset from the nominal position of the 2P-MMR. Even though the n_1/n_2 separation stays fixed at ∼1.51, the outer pair continues its convergent migration. In the space of separations, this means that the triplet moves vertically and downwards.

This behaviour is expected from a triplet with masses that meet the condition for convergent migration (Beaugé & Cerioni, 2022). Given our adopted disk, this condition translates to outer planets being more massive than inner planets. For this work, we focus on the moment where triplets cross the $(4, -7, 3)$ and $(2, -4, 3)$ 3P-MMR, to check whether they get captured or continue their path past them.

We observe the following results from Fig. 1. The grid cells can be divided into two camps. Out of the 100 total systems, 43 of them converged to the $(2, -4, 3)$, at least temporarily, while the other 57 did not get captured in any of the 3P-MMRs. The red-colored domain suggests that a capture in the $(2, -4, 3)$ resonance is the most expected outcome in some given region of the initial separation space, and not just a few scattered solutions resulting from finely tuned initial conditions. A determining factor for the capture seems to be the initial separation of the outer pair, which in this case has to be greater than $n_2/n_3 \sim 3.6$. Lastly, we did not get any captures of the $(4, -7, 3)$ 0th-order 3P-MMR.

The fact that a capture in the 1st-order 3P-MMR is more likely than the 0th-order one is striking, given that both can be a consequence of the $(3/2\,,\,3/1)$ 2P-MMR coupling. The reasons for this preference seem complex and will be further explored in a future study.

Next, we present how these results change upon variations of planetary and disk parameters.

3.2. Changing planetary parameters

Our adopted planetary migration rates, as modelled by Tanaka & Ward (2004), depend upon planetary param-

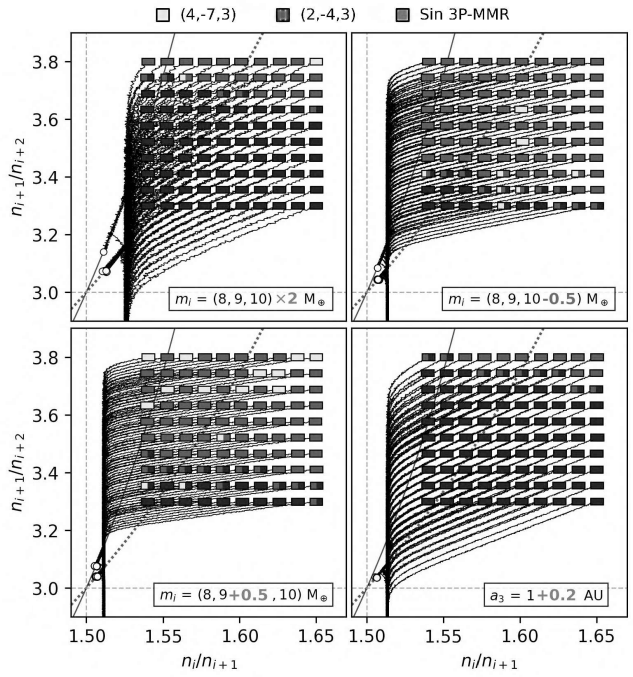

Fig. 2. Analogous to Fig. 1 but changing planetary parameters, as indicated in each legend.

eters as $m_i\, a_i^{(0.5-s-2f)}$. Meaning, for example, that a more massive planet would fall inwards more rapidly. In Section 2.1 we adopted $(s, f) = (0.5, 0)$, so we expect the planetary masses to be particularly decisive for the convergence and capture of the triplets.

In Fig. 2 we show grids analogous to that of the previous section, but this time changing initial conditions on planetary masses and semimajor axes. In the upper left plot we adopt planets with double the mass of those in our standard system (Fig. 1), i.e (16,18,20) $M_\oplus$. Migration rates will therefore be accelerated in comparison, though the *relative* masses and migration rates should stay the same. Either way, we see that the red-colored convergence domain of the $(2, -4, 3)$ has reduced to only 27 systems, pushing the interface upwards towards $n_2/n_3 \sim 3.7$. This could be due to dynamical effects that depend on the absolute values of the masses, such as the resonant offset which separate planetary pair from the 3:2 2P-MMR. We also find some captures in the $(4, -7, 3)$ resonance, marked by the yellow boxes. There is even a case which shows a temporal capture in the $(4, -7, 3)$ followed by a capture in the $(2, -4, 3)$ (the red and yellow box).

In the upper right plot we reduce the mass of the third planet to $m_3 = 9.5\, M_\oplus$. The convergence of a resonant chain is specially sensitive to the mass of the last (and also the first) planet (Beaugé & Cerioni, 2022). For a Type-I migration scheme, a more massive planets favours the formation of a resonant chain, although not necessarily to the $(2, -4, 3)$ resonance, as we can see in this case. When comparing it with 1, we learn that having a less massive third planet produced more captures in the 1st-order 3P-MMR. Considering the lower left plot as well, which uses a more massive second planet, we conclude that an important factor for the 1st-order 3P-MMR capture is that the difference between m_2 and m_3 be small, while still meeting the convergence mass conditions. Additional testing showed that changes in the mass of the first planet do not affect the results as significantly as changes in the mass of the outer two.

On the other hand, we analyzed the lower right plot where we widen the orbits by fixing the initial value of a_3 at 1.2 AU. We recall that each cell fixes initial relative separations, so only one initial semimajor axis has to be assigned in order to calculate the rest. In this way, we are testing wider initial orbits. Contrary to our expectations at the beginning of this section, it seems that inidividual semimajor axes and the overall initial scale of the system do affect the capture domain. A slightly wider system appears to reduce considerably the amount of convergent systems. Because migration rates are, in theory, independent of semimajor axes, we suspect that the difference lies in mutual gravitational interactions, given that these are in fact smaller as the planets are farther from each other.

Lastly, we observe that those systems which converged to the $(4, -7, 3)$ 3P-MMR are few and scattered over a smooth red-colored domain in separation space in which the systems consistently converge to the higher orden 3P-MMR. Indeed, a capture in the $(2, -4, 3)$ resonance appears significantly more probable than one in the $(4, -7, 3)$ in our simulations.

We ran further tests and saw that variations of *other* planetary parameters, such as initial excentricities, mean anomalies and longitudes of node do not affect the migration paths presented.

3.3. Changing disk parameters

In Section 2.1 we showed that the gas disk adopted in our simulations is parametrized by (Σ_0, s, H_0, f). In Fig. 3 we repeat the analysis of the previous section, this time varying disk parameters.

We find that the convergence domain is highly sensitive to small changes in the disk. While other works in the literature often adopt Σ_0 values in the order of $\sim 10^3$ gr cm^{-2}(Weidenschilling, 1977; Garaud & Lin, 2007; Hirose & Turner, 2011), we find that a small increase of 25 gr cm^{-2} reduces significantly the amount of convergent systems (upper left plot). Additional testing with $\Sigma_0 = 150$ gr cm^{-2} result in no captures at all. It has been shown that higher disk densities lead to captures in ever more compact resonances (Kajtazi et al., 2023), and in this case, it is crucial that the outer pair becomes captured in the rather wide configuration of the 3:1 2P-MMR.

Convergence seems to be even more sensitive to small changes in parameter s. The radius power of the surface density distribution is usually given values between $s \in [0.5, 1.5]$ (Miotello et al., 2018). In the upper right plot of Fig. 3 we see that a value slightly greater than $s = 0.5$ allows every single system to be captured in a 3P-MMR, although two of them do eventually escape. High sensitivity upon small changes in disk parameters is also observed in the lower plots, where we slightly increase the disk aspect ratio H_0 and flare f.

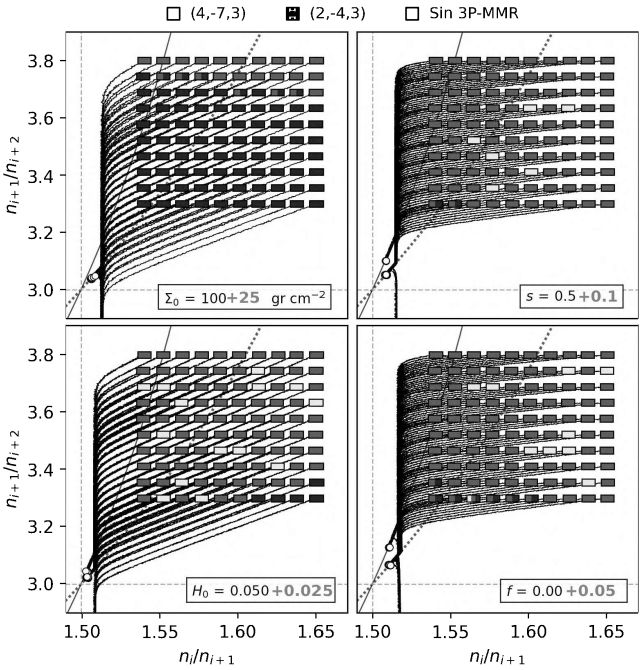

Fig. 3. Analogous to Fig. 1 but changing disk parameters, as indicated in each legend.

Lastly, we once again find that captures in the $(4, -7, 3)$ resonance are few and sparse, in stark contrast to the $(2, -4, 3)$, which dominates the convergence domain in robust fashion.

4. Conclusions

We have recently presented dynamical evidence suggesting, for the first time, the effects of a 1st-order 3-planet mean-motion resonance in a real planetary system (K2-138, Cerioni & Beaugé, 2023). In this work, our goal was to analyze which conditions favour the capture in such a theoretically weak 3P-MMR. To this end, we studied the capture conditions of a planetary triplet of 8, 9 and 10 $M_\oplus$ in the 1st-order 3P-MMR $(2, -4, 3)$, which can take place after a migration process which carries the planets towards an intersection of 3:2 and 3:1 2P-MMRs between the inner and outer pair, respectively. This migration story is believed to have happened among the K2-138 e, f and g planets.

To this end, we ran a grid of simulations with different initial separations between the planets. Then, we used these results as a comparison standard with which we can determine how small changes in planetary and disk parameters affect the capture in the 3P-MMR.

As a result, we observed the following general trends. On one hand, the capture does depend on initial relative separations, being particularly sensitive to that of the outer planetary pair. On the other hand, we find that the $(2, -4, 3)$ resonance dominates the convergence region, in contrast to the $(4, -7, 3)$, which accumulates sparse captures with no visible structure in mean-motion-ratio space, in spite of being a lower order 3P-MMR which can also result from the (3/2,3/1) 2P-MMR coupling. Additionally, we find that the capture in the 1st-order 3P-MMR is specially sensitive to even small changes in the disk.

Furthermore, we find that the $(2, -4, 3)$ capture is favoured by:

- a greater initial separation between the outer planetary pair.
- small planetary masses, as long as they meet the convergence mass conditions. This trend is only valid down to a few Earth masses. A test of (8,9,10) M_{mars} resulted in very few captures.
- similar masses between the second and third planet, as long as they meet the convergence mass conditions. Although a high mass on the third planet gives better odds for forming a resonant chain (Beaugé & Cerioni, 2022), it actually prevents the capture in the $(2, -4, 3)$ resonance specifically.
- small initial semimajor axes.
- a smaller disk surface density at $r = 1$ AU Σ_0.
- a greater disk radius surface density power s.
- a greater disk aspect ratio at $r = 1$ AU H_0.
- a greater disk flare f value.

Our results spark other questions such as why is the initial separation between the planets such a determining factor for the $(2, -4, 3)$ capture even when every system crosses the $(n_1/n_2, n_2/n_3) = (3/2, 3/1)$ intersection? What's more, why do these triplets get captured in the 1st-order 3P-MMR rather than the 0th-order one which is also associated with that intersection? Although these questions exceed the scale of this work, one hypothesis could be related to the different topology found in both resonances (Petit, 2021).

Acknowledgements: The authors would like to thank IATE for providing the necessary computing power that carried the presented simulations.

References

Agol E., et al., 2021, Planet. Sci. J, 2, 1
Beaugé C., Cerioni M., 2022, CeMDA, 134, 57
Bulirsch R., Stoer J., 1966, Numer. Math., 8, 1
Cerioni M., Beaugé C., 2023, ApJ, 954, 57
Garaud P., Lin D.N.C., 2007, ApJ, 654, 606
Hirose S., Turner N.J., 2011, ApJL, 732, L30
Hühn L.A., et al., 2021, A&A, 656, A115
Kajtazi K., Petit A.C., Johansen A., 2023, A&A, 669, A44
Leleu A., et al., 2021, A&A, 649, A26
Miotello A., et al., 2018, A&A, 619, A113
Petit A.C., 2021, Celestial Mechanics and Dynamical Astronomy, 133, 39
Tanaka H., Takeuchi T., Ward W.R., 2002, ApJ, 565, 1257
Tanaka H., Ward W.R., 2004, ApJ, 602, 388
Weidenschilling S.J., 1977, Ap&SS, 51, 153